Journal of Catalysis 280 (2011) 161–167

Contents lists available at ScienceDirect

Journal of Catalysis

journal homepage: www.elsevier.com/locate/jcat

NO_x storage and reduction over potassium titanate nanobelt-based catalyst with high storage capacity

Weihua Shen, Atsue Nitta, Zhi Chen, Tomonori Eda, Akihiro Yoshida, Shuichi Naito *

Department of Material and Life Chemistry, Kanagawa University, 3-27-1, Rokkakubashi, Kanagawa-ku, Yokohama 221-8686, Japan

ARTICLE INFO

Article history:
Received 11 December 2010
Revised 17 March 2011
Accepted 18 March 2011
Available online 22 April 2011

Keywords:
NO_x storage/reduction
Potassium titanate
Nanobelt
Platinum
$K_2Ti_8O_{17}$

ABSTRACT

We have identified a new NO_x storage/reduction catalyst with the composition of Pt–KNO_3 supported on a K-titanate nanobelt (KTN) prepared using hydrothermal method. Isothermal NO_x storage experiments at 350 °C revealed the highest storage capacity (2.27 mmol/g) ever achieved over 33 wt.% KNO_3 impregnated catalyst, and lean–rich cycles could be operated for more than 15 times with maintaining its high storage capacity. The characterization of the spent catalysts revealed that addition of more than 33 wt.% KNO_3 caused the gradual destruction of the nanobelt structure during the reaction and the decrease in NO_x storage capacity. High temperature operation such as at 500 °C also caused the destruction of nanobelt structure. It was demonstrated that the main storage specie of NO_x was potassium nitrate. Immigration of K^+ from and back to K-rich layers on KTN might be the mechanism for the storage and reduction of NO_x on those materials.

1. Introduction

Emissions of NO_x to the atmosphere can cause various environmental problems. Therefore, NO_x emissions must be strictly controlled and regulated [1,2]. On the other hand, because of the limited resources of crude oil in the world and increasingly severe global warming, developments of fuel-efficient vehicles have long been continued. Most current gasoline-burning engines operate under a very narrow air-to-fuel ratio (A/F) range near the stoichiometric value (A/F = 14.7, rich-burn) with little or no O_2 in the exhaust, but lean-burn engines (A/F = 20–25) can burn fuel more efficiently [3,4]. However, conventional three-way catalysts are ineffective for NO_x removal under an oxidative atmosphere. For that reason, an effective NO_x removal technique for lean-burn exhaust becomes desirable from both environmental and catalytic perspectives. In fact, NO_x removal technologies under the lean-burn condition include direct catalytic decomposition of NO_x [5], catalytic NO_x storage/reduction (NSR) [2,6–9], and selective catalytic reduction of NO_x with urea/NH_3 [10,11] or hydrocarbon [12–14].

The NSR catalysts are operated under cyclic fuel-lean fuel-rich condition. Under lean-burn condition, NO_x is absorbed on the catalyst; and under rich-burn condition, the stored NO_x is reduced by H_2, CO, and hydrocarbons. Generally, the NSR catalysts contain three compositions: a high surface area metal oxide such as Al_2O_3 as a support, basic elements such as Ba and K as the NO_x storage sites, and precious metals such as Pt, Pd, and Rh as the redox sites for oxidizing NO to NO_2 and reducing the stored NO_x to regenerate storage capacity. In real systems, the storage period of 1–2 min followed by 3–5 s rich conditions is typically adopted. The model NSR catalyst is Pt–Ba/Al_2O_3, which has been developed by Toyota's research group [6–9]. Although considerable amounts of experimental and theoretical investigations of Pt–Ba/Al_2O_3 have been reported, severe problems have been unsolved with respect to sulfur poisoning [8,15–18]. Meanwhile, NSR catalysts with high NO_x storage capacity are desirable because increasing the NO_x storage capacity can decrease the necessary amount of catalyst and thereby decrease the amount of precious metal and costs.

Aside from Al_2O_3, titanium oxide has been proposed as an efficient support because of its higher resistance to sulfur poisoning than typical Al_2O_3 [8]. Previous reports have demonstrated that K-based catalyst showed good performance on NO_x storage in a lean-burn atmosphere [19–22]. Most researchers believe that the reaction of K with titania will cause the loss of NO_x storage capacity. However, recent studies of $K_2Ti_2O_5$, prepared through a solid state reaction, showed high NO_x storage capacity (1.2 mmol/g), which was achieved on Pt/$K_2Ti_2O_5$ at 550 °C [23,24]. The structural transformation between $K_2Ti_2O_5$ and $K_2TI_6O_{13}$ has been regarded as the mechanism for NO_x storage on Pt/$K_2Ti_2O_5$ [24]. The lower NO_x storage capacity at lower temperature (200–400 °C) as well as the slower NO_x storage rate even at higher temperatures (550 °C) has limited the application of $K_2Ti_2O_5$-based catalysts in wide areas.

Alkali titanate nanomaterials have been widely investigated [25–29]. However, the usual applications of such kind nanomaterials

* Corresponding author. Fax: +81 45 413 9770.
E-mail address: naitos01@kanagawa-u.ac.jp (S. Naito).

0021-9517/$ - see front matter © 2011 Elsevier Inc. All rights reserved.
doi:10.1016/j.jcat.2011.03.014

have specifically addressed the formation of titania nanomaterials by neutralizing them with acid [30–32]. Here, we present the preparation of K-titanate nanobelt (KTN) and its use as a support for NSR reaction. For characterization, X-ray diffraction (XRD), X-ray photoelectron spectroscopy (XPS), N_2 sorption measurement, and transmission electron microscope (TEM) techniques were used. Isothermal NO_x storage and lean–rich cycling test were used for the characterization of NO_x storage performance. The prepared Pt–KNO_3/KTN showed the highest NO_x storage capacity at 350 °C reported so far. A possible mechanism based on the formation of a K-rich layer on the nanobelt was proposed.

2. Experimental

2.1. Preparation of catalysts

The KTN was prepared by hydrothermal treatment using TiO_2 and KOH as the starting materials. The preparation method was similar to that described in a previous report [29], except that commercial TiO_2 (P-25; Japan Aerosol Corp.) was used in this work. In detail, 3 g of TiO_2 was added to 100 mL of 10 mol/L KOH aqueous solution. After being stirred for 30 min, the resultant suspension was transferred to an autoclave. Then the autoclave was sealed and heated at 130 °C for 4 days. After the autoclave cooled down to room temperature, the white solid product was collected by filtration, washed several times with deionized water, and dried overnight at 100 °C. Various amounts (0, 20, 26, 33, and 41 wt.%) of KNO_3 and 1.5 wt.% Pt were dispersed onto KTN by conventional impregnation method with aqueous H_2PtCl_6 and KNO_3 mixed solutions. The mixtures were put into an oven at 70 °C until the water evaporated. Finally, the impregnated samples were calcined at 350 °C for 2 h and designated as Pt–*xx*KNO_3/KTN, where *xx*% signified the weight percent of KNO_3.

2.2. Procedure for catalytic tests

Catalytic tests were performed on a fixed-bed gas-flow reactor equipped with a pulse gas feed system. The outlet gas was analyzed by an online quadruple mass spectrometer (QMS QME200; Pfeiffer). The experimental conditions used for the catalytic tests are presented in Table 1. Prior to each catalytic test, the catalyst was reduced by 80 mL/min 8% H_2/He flow in a quartz tube reactor from room temperature to 350 °C with a ramp rate of 10 °C/min and maintained at 350 °C for 30 min. During this procedure, the outlet gas was analyzed using QMS and the data were used for temperature program reduction (TPR) profiles. The QMS signals assigned to gas components were as follows: H_2 ($m/e = 2$), He ($m/e = 4$), NH_3 ($m/e = 15$), H_2O ($m/e = 18$), N_2 ($m/e = 28$), NO ($m/e = 30$), N_2O ($m/e = 44$), and NO_2 ($m/e = 46$). For analyses, the signal intensity of He was applied as a reference to calculate the relative signal intensity of other gases. For example, the relative signal intensity of H_2 was calculated as $I_{m/e=2}/I_{m/e=4}$.

Table 1
Experimental conditions employed in this work.

Procedures	Experimental condition
(i) NO_x isothermal test	NO_x storage: 930 ppm NO + 7% O_2 in He, 80 mL/min; H_2 reduction: 4% H_2 in He, 80 mL/min; 100 mg catalyst
(ii) Lean–rich cycling test (1)	Lean: 930 ppm NO + 7% O_2 in He, 160 mL/min, 6 min; Rich: 4% H_2 in He, 160 mL/min, 4 min; 50 mg catalyst
(iii) Lean–rich cycling test (2)	Lean: 930 ppm NO + 7% O_2 in He, 160 mL/min, 3 min; Rich: 930 ppm NO + 4% H_2 in He, 160 mL/min, 30 s; 50 mg catalyst

For the isothermal NO_x storage test, 80 mL/min of 930 ppm NO/7% O_2/He was flowed through 100 mg of catalyst at 350 °C. Meanwhile, the outlet gas was analyzed using QMS. After being flushed by 80 mL/min of He for 15 min, the NO_x storage catalyst was then reduced by 80 mL/min of 4% H_2/He at 350 °C and the outlet gas was analyzed using QMS. The processes described above were repeated. The data obtained from the second time test was then used for analyses. In some cases, the catalysts with NO_x storage were removed from the reactor and used as samples for thermal-gravity (TG) experiments. The NO_x storage capacities of the catalysts were calculated using both the QMS data and TG results.

The TG experiments (Thermo Plus TG 8120; Rigaku Corp.) were adopted to confirm the NO_x storage capacities. About 5 mg of the spent catalyst with NO_x storage was used as sample for each experiment. The sample was heated from room temperature to 300 °C with a ramp rate of 10 °C/min under 200 mL/min of He and maintained at 300 °C. While the temperature was maintained, the gas flow was switched from He to 5% H_2/He. The weight loss after the gas switching was collected and was utilized for the calculation of NO_x storage capacity.

For lean–rich cycling tests, 50 mg of catalyst was used. Lean–rich cycles at 350 °C (lean: 6 min of 930 ppm NO/7% O_2/He, and rich: 4 min of 4% H_2/He with 160 L/min flow rate) were used to check the kinetic property and stability of the catalysts. To investigate the NO reduction during regeneration process, 930 ppm NO/4% H_2/He was also used as gas feed during rich-burn process. In this case, the lean–rich cycling test was operated on 50 mg of Pt–26KNO_3/KTN catalyst at 350 °C under the following cyclic gas feed: 3 min of 160 mL/min 930 ppm NO/7% O_2/He, and 30 s of 160 mL/min 930 ppm NO/4% H_2/He.

2.3. Characterizations

The XRD pattern was recorded on (MultiFlex 2KW; Rigaku Corp.) using Cu Kα1 source with 40 kV and 20 mA. The TEM observations were conducted on (JEM-2010; JEOL) with 200 kV accelerating voltage. The N_2 sorption measurement was conducted by Tristar 3000 (Micromeritics Instrument Corp.) at liquid nitrogen temperature. Prior to each N_2 sorption measurement, the sample was degassed in vacuum at 250 °C for 1 h. The specific surface area was calculated using the Brunauer–Emmett–Teller (BET) method. The XPS was taken on (JPM-9010MC; JEOL) with a Mg Kα1 source. The XPS apparatus has a preparation chamber in which the sample can be heated in situ and reduced by hydrogen. A pressed disc was used for XPS measurement. The C1s (284.3 eV) peak was used as the standard reference of binding energies.

3. Results and discussion

3.1. NO_x storage and reduction

The crystal structure of the prepared KTN was analyzed using XRD. All reflection peaks of prepared KTN in Fig. 1a can be assigned to a monoclinic phase of $K_2Ti_8O_{17}$ (JCPD No. 84-2057), indicating that the TiO_2 was transformed completely into potassium titanate. The (0 2 0) peak was higher and much narrower than other peaks, suggesting the high orientation of the nanostructure [29]. Fig. 1b presents a typical TEM image of the prepared KTN. The $K_2Ti_8O_{17}$ nanobelts of several micrometers in length and tens of nanometers in width were observed in bending and twisting features. From XRD and TEM results, it was able to conclude that uniform nanobelt with a composition of $K_2Ti_8O_{17}$ was prepared successfully. The N_2 sorption measurement showed that the prepared KTN has

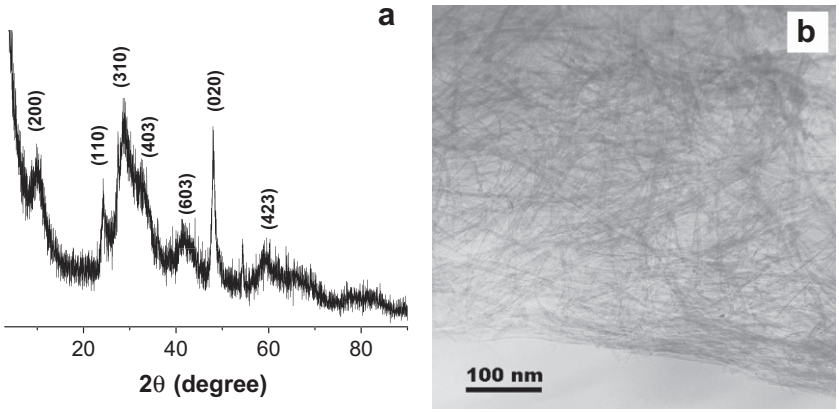

Fig. 1. (a) XRD pattern and (b) TEM image of as-prepared KTN.

a BET surface area as high as 284 m^2/g. All the TPR profiles of the Pt–KNO_3/KTN catalysts were similar. A typical TPR profile of Pt–26KNO_3/KTN is presented in Fig. 2. Results show that the impregnated KNO_3 was reduced with the presence of Pt by H_2 at the temperatures of 150–170 °C, accompanied with the consumption of H_2 and the formation of N_2, H_2O, and small amount of NH_3.

Fig. 3 shows the time courses of isothermal NO_x storage on varied catalysts at 350 °C. The storage process includes two stages: at the first stage, the NO_x was completely trapped, no outlet NO being detected; and at the second stage, NO_x was partially trapped, the outlet NO being increased concomitantly with time. As depicted in Fig. 3, with the increasing amount of impregnated KNO_3, the time when NO_x was trapped completely increased significantly from 5 min (for Pt/KTN) to the maximal 34 min (for Pt–33KNO_3/KTN) and then decreased to 20 min (for Pt–41KNO_3/KTN). No other nitrogen species such as NO_2 and N_2O were detected. Therefore, the different NO concentrations between the input and outlet gases were attributed to the NO_x storage on the catalyst. The NO_x storage capacities calculated from the isothermal NO_x storage experiment are presented in Table 2. Although the prepared Pt/KTN showed some NO_x storage properties, its storage capacity was the lowest (0.36 mmol/g). Results show that the NO_x storage capacity increased dramatically with the addition of KNO_3. The maximal NO_x storage capacity was achieved on Pt–33KNO_3/KTN (2.41 mmol/g). Fig. 4 shows the reduction process of stored NO_x on Pt–26KNO_3/KTN by 4% H_2/He. During the first 4 min, H_2 was consumed completely by the following reaction: $NO_x + xH_2 \rightarrow xH_2O + 1/2N_2$. The main reduced products were N_2 and H_2O, almost no other nitrogen species being detected during this process. The isothermal NO_x storage experiment on Pt–26KNO_3/KTN was also conducted at 500 °C, as shown in Supporting information (SI, Fig. s1). The NO_x storage capacity was 0.90 mmol/g at 500 °C. The TEM observation (SI, Fig. s2) indicated the destruction of nanobelt structure had taken place during the reaction at 500 °C. Therefore, the thermal stability should be improved to promote K-titanate nanomaterial as NSR catalyst operated at high temperature.

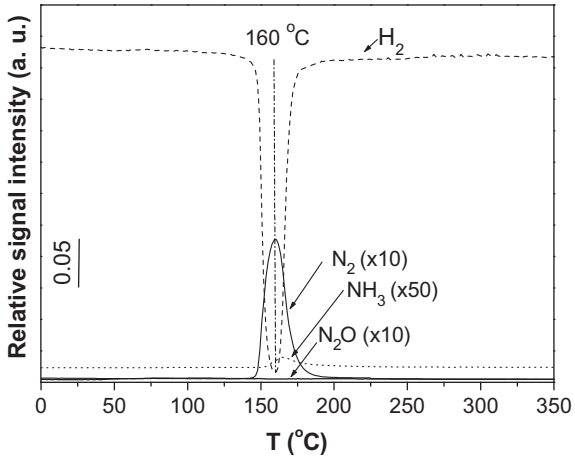

Fig. 2. TPR profile of Pt–26KNO_3/KTN (100 mg sample in 80 mL/min 8% H_2/He with 10 °C/min temperature ramp rate).

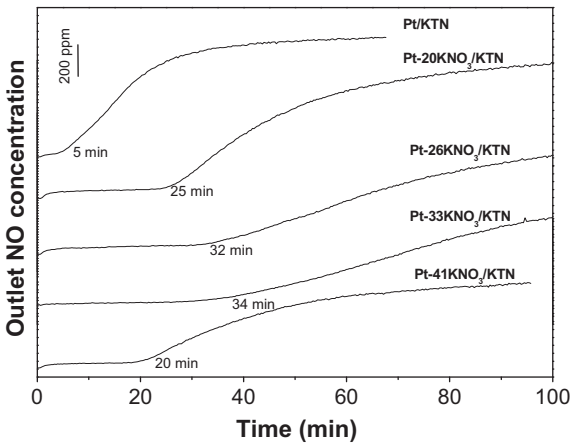

Fig. 3. Time courses of the outlet NO concentration on different catalysts during isothermal NO_x storage test at 350 °C (100 mg sample, 80 mL/min 930 ppm NO/7% O_2/He).

The TG experiments of the spent catalysts with NO_x storage were conducted to confirm the NO_x storage capacities. Fig. 5 shows that the weight losses are observed immediately after the gas flow switched from He to 5% H_2/He at 300 °C. If we assume that the chemical state of N among the stored NO_x is +5, then the NO_x storage species can be considered as KNO_3. Therefore, the reaction between stored NO_x and H_2 can be described as follows: $2KNO_3 + 5H_2 \rightarrow K_2O + N_2 + 5H_2O$. Because the formed N_2 and H_2O are released as gases at 300 °C, the weight loss can be considered as resulting from the removal of N_2O_5. For 1 g of spent catalyst, the weight amount of N_2O_5 is $1 * wl\%/100\%$ (g) (where wl% means weight loss%). The molecular weight of N_2O_5 is 108 (g/mol). Therefore, the molar amount of N_2O_5 in 1 g of spent catalyst is $1 * wl\%/100\%/108$ (mol); the molar amount of nitrogen is $1 * wl\%/100\%/108 * 2 = 1 * wl\%/100\%/54$ (mol). Finally, the NO_x storage capacity calculated from the TG results can be written as $wl\%/100\%/54 * 1000$ (mmol/g). If the real chemical state of N among the

Table 2
Surface areas and NO_x storage capacities at 350 °C of Pt–KNO_3/KTN catalysts.

Catalysts	BET-specific surface area (m^2/g)			NO_x Cap. (mmol/g)		K/Ti[a]	NO_x/K%[b]
	As-prep.	A.R.(NO_x)	A.R.(H_2)	QMS	TG		
Pt/KTN				0.36	0.25	0.25	9
Pt–20KNO_3/KTN	164	148	164	1.57	1.27	0.48	31
Pt–26KNO_3/KTN	130	110	128	2.04	1.95	0.57	42
Pt–33KNO_3/KTN	113	81	88	2.41	2.27	0.70	44
Pt–41KNO_3/KTN	73	31	40	1.52	1.31	0.89	23

As-prep. = as-prepared, A.R.(NO_x) = after reaction with NO_x storage, and A.R.(H_2) = after reaction with H_2 reduction.
[a] The composition of the KTN was considered as $K_2Ti_8O_{17}$.
[b] The NO_x storage capacity calculated from TG experiment was used for this calculation.

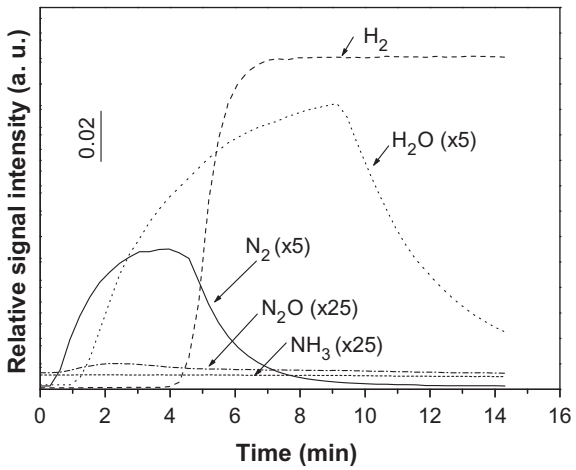

Fig. 4. Time courses of the reduction process of stored NO_x on Pt–26KNO_3/KTN catalyst at 350 °C (100 mg catalyst, 80 mL/min 4% H_2/He).

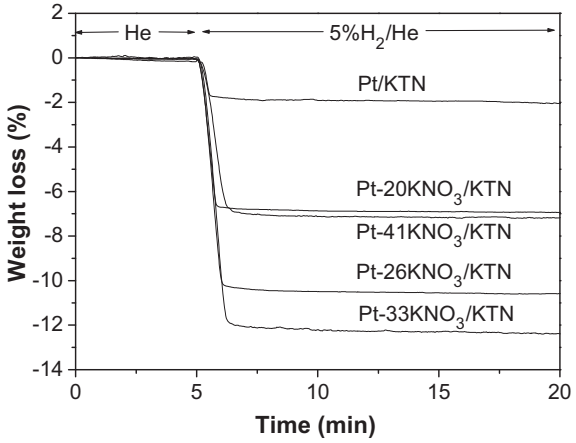

Fig. 5. TG profiles of spent catalysts in NO_x storage state (about 5 mg sample, 200 mL/min gas flow, and at 300 °C).

stored NO_x is less than +5, it can be readily deduced that the calculated NO_x storage capacity from the above equation is less than the actual capacity. The results of these calculations for spent catalysts are presented in Table 2, from which it is apparent that the NO_x storage capacity increased significantly with the impregnation of KNO_3 and that the storage capacity increased concomitantly with the increasing amount of impregnated KNO_3 until 33 wt.% and then decreased. Table 2 also shows that the NO_x storage capacity of each catalyst calculated from TG is comparable with that calculated from the QMS data. To the best of our knowledge, the NO_x storage capacity of 2.27 mmol/g (calculated from TG) in the case of Pt–33KNO_3/KTN is the highest value ever reported in the literature. It is more than twice that of Pt–Ba/Al_2O_3 [2].

To evaluate the NO_x storage rate and stability of the catalysts more deeply, lean–rich cycling tests were conducted (depicted in Fig. 6). During the NO_x storage process, NO was first oxidized to NO_2 on Pt and stored on potassium site as KNO_3. The stored NO_x was then reduced by H_2 in the presence of Pt during reduction procedure. Fig. 6a shows that the flowed H_2 was consumed completely during the first 1 min, followed by increasing gradually during reduction process. The main products during reduction were N_2 and H_2O, neither N_2O nor NH_3 being detected. As depicted in Fig. 6b, the outlet NO amounts over varied Pt–KNO_3/KTN catalysts decreased concomitantly with the increasing amount of impregnated KNO_3, showing the minimum at 26–33% impregnation, and increased again on Pt–41KNO_3/KTN. Almost no NO was emitted in the case of Pt–26KNO_3/KTN and Pt–33KNO_3/KTN, suggesting that these two catalysts have rapid storage rates as well as high

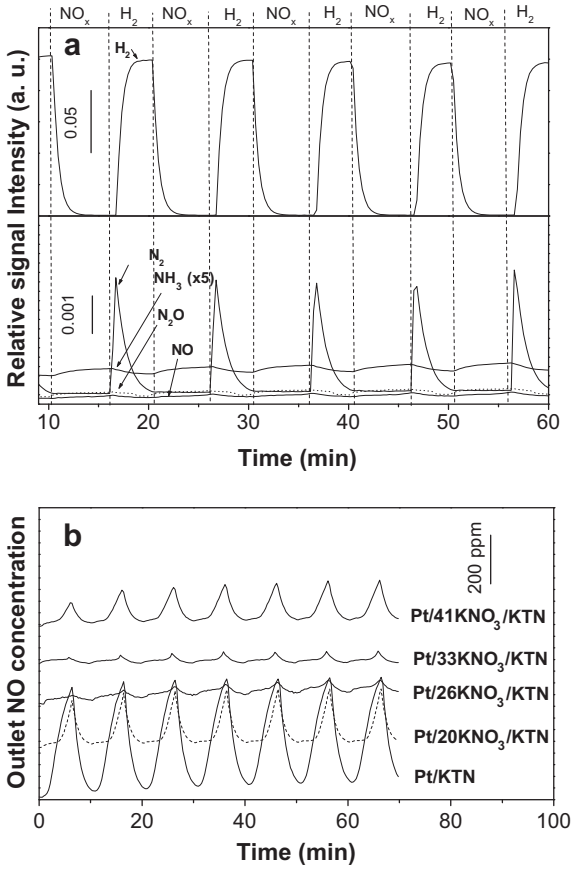

Fig. 6. Lean–rich cycling tests (1): (a) on Pt–26KNO_3/KTN, and (b) outlet NO concentrations on different catalysts (50 mg catalyst) at 350 °C.

storage capacities. The optimal amount of KNO_3 impregnation is 26–33 wt.% from the result of isothermal NO_x storage experiments and lean–rich cycling tests. During rich procedure on Pt–26KNO_3/KTN, 930 ppm NO/4% H_2/He was also employed as gas feed, as shown in Fig. 7. During the lean condition, the NO_x was completely absorbed for 3 min and emitted NO was undetected. During the rich condition, the stored NO_x was reduced to N_2 and no outlet NO was detected, indicating that this catalyst was also effective for the reduction of NO by H_2 during the rich condition.

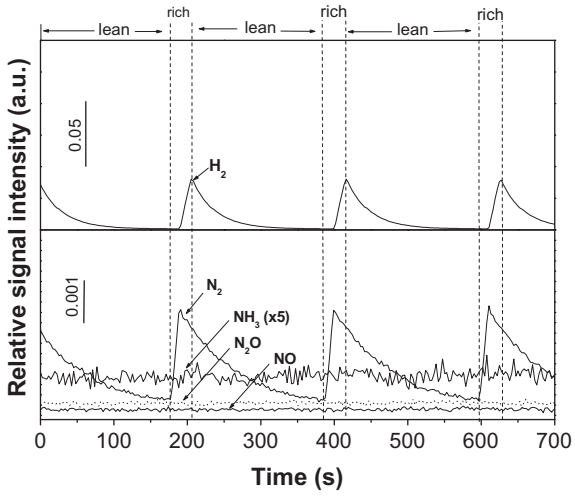

Fig. 7. Lean–rich cycling test (2) on 50 mg of Pt–26KNO_3/KTN at 350 °C.

3.2. Characterizations

Fig. 8 shows the TEM images of the spent catalysts after H_2 reduction. The Pt was highly dispersed on every catalyst with the particle sizes around 1–2 nm. When the amount of impregnated KNO_3 was less than 26%, the nanobelt structure was maintained completely after the reaction. However, some nanobelts were transformed into irregular potassium titanate particles in the case of spent Pt–33KNO_3/KTN catalysts. Most of the nanobelts were destroyed on spent Pt–41KNO_3/KTN. Combining the results of isothermal NO_x storage experiment and TEM observation, it was concluded that the preservation of the nanobelt structure as well as addition of suitable amounts of KNO_3 were the key factors to obtain high NO_x storage capacity.

The BET-specific surface areas of the catalysts are presented in Table 2. The BET-specific surface area of the as-prepared catalyst was decreased with the increase in the impregnated KNO_3 amount because KNO_3 addition will increase the total weight. The BET-specific surface area of each catalyst decreased after the reaction. Because the stored NO_x increases the total weight, the surface area of the spent catalyst with NO_x storage state is lower than that with reduction state. The decreasing extent of the surface area of spent catalyst was increased with the increase in KNO_3 impregnation amount, especially in the case of Pt–41KNO_3/KTN (only half was maintained after reaction). The result of N_2 sorption confirmed that the nanobelt structure of Pt–KNO_3/KTN was maintained after

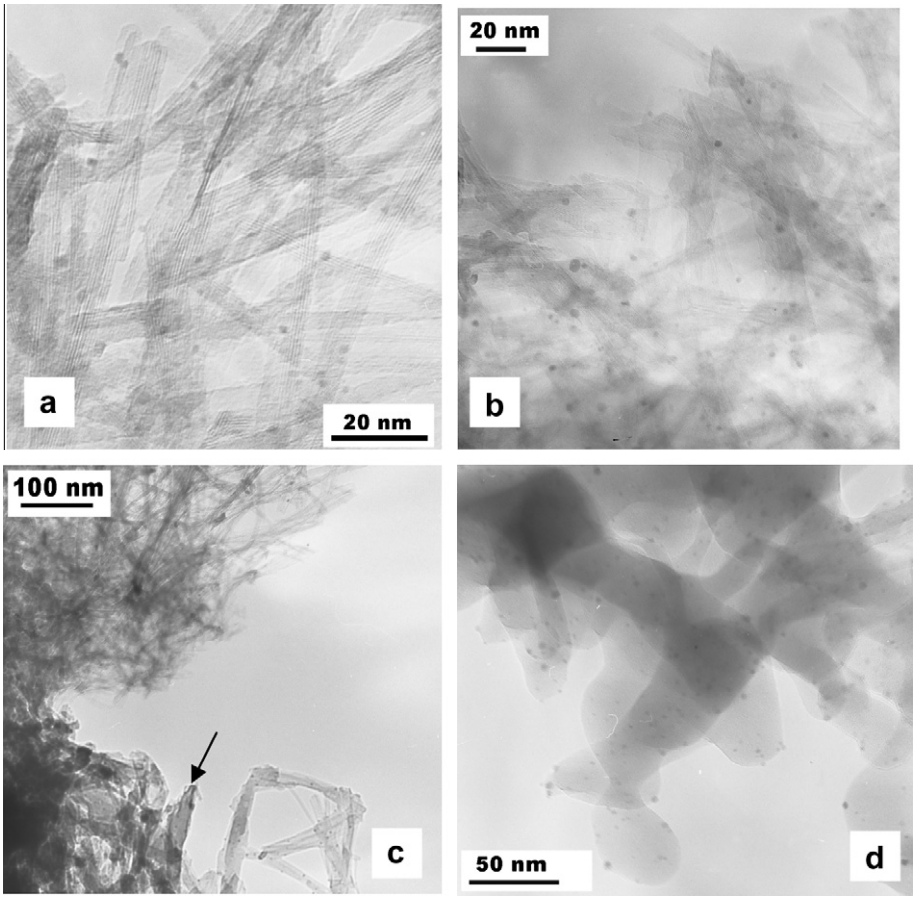

Fig. 8. TEM images of spent catalysts after H_2 reduction: (a) Pt–20KNO_3/KTN, (b) Pt–26KNO_3/KTN, (c) Pt–33KNO_3/KTN (arrow head shows fusion of the nanobelts), and (d) Pt–41KNO_3/KTN.

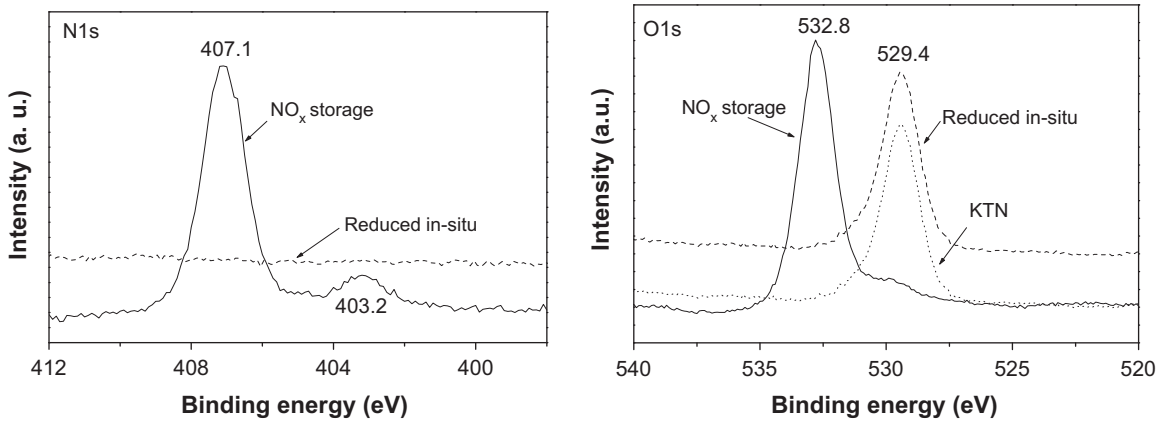

Fig. 9. XPS spectra of as-prepared KTN, and spent Pt–20KNO_3/KTN in the NO_x storage state and reduced state in situ by H_2.

reaction when the lower KNO_3 amount was modified and was destroyed when the higher KNO_3 amount was modified.

Fig. 9 shows the XPS results of as-prepared KTN, the spent Pt–20KNO_3/KTN catalyst in NO_x *at* the storage state, and the reduced state in situ by H_2. The N1s transition of spent catalyst with NO_x storage state shows two peaks with the binding energy at 407.1 eV (mainly) and 403.2 eV, which can be assigned to KNO_3 and KNO_2, respectively. Those two peaks disappeared after in situ H_2 reduction, indicating the complete reduction of NO_x by H_2. The O1s at 532.8 eV is attributed to the KNO_3 and/or KNO_2. Compared with as-prepared KTN, the peak at 529.4 eV can be attributed to potassium titanate. The O1s transition of spent catalyst with NO_x storage has a main peak with the binding energy at 532.8 eV and a weak shoulder with the binding energy at 529.4 eV, suggesting that the stored NO_x species covered the entire surface of nanobelts. Because of the removal of the NO_x covering, the KNO_3 peak at 532.8 eV disappeared after in situ reduction. Meanwhile, the former shoulder assigned to potassium titanate at 529.4 eV became the main peak and the intensity increased greatly. From these observations, we can conclude that the stored NO_x species is mainly KNO_3 and that almost all surface of catalyst is covered by KNO_3.

Fig. 10 presents XRD patterns of Pt–26KNO_3/KTN catalysts. The as-prepared catalyst presents some additional reflection peaks beside the XRD reflection of KTN, with especially clear reflection peaks at 23.5° and 27.2°, which could be assigned to the orthorhombic and hexagonal phases of KNO_3, respectively. The intensity of the peak at 27.2° increased concomitantly with the increase in KNO_3 loading amounts on as-prepared catalysts (not shown). The reflection peaks at 23.5° and 27.2° disappeared after reduction, confirming that these peaks were assigned to KNO_3. Two additional peaks at 27.7° and 30.7° appeared on the reduced Pt–26KNO_3/KTN. Although we can not exactly assign those two peaks, they may be originated from some K-rich titanate (K/Ti > 2/8). Once NO_x was absorbed, the reflection peaks at 23.5° and 27.2° appeared again, indicating that the species of stored NO_x was KNO_3. The intensity of these KNO_3 peaks in NO_x storage state of the spent catalysts increased concomitantly with the increase in KNO_3 loading amount and then decreased in the case of Pt–41KNO_3/KTN (not shown), which corresponds well to the NO_x storage amount calculated from QMS and/or TG result.

Because potassium cations are surrounded by titanium oxide units in K-titanate with low K/Ti ratio such as $K_2Ti_8O_{17}$ and $K_2Ti_6O_{13}$, the chemical activity of potassium is considered to be inert. However, potassium may possess chemical activity with high K/Ti ratios such as $K_2Ti_2O_5$, in which titanium oxide units form tunnels [23,24]. The prepared Pt/KTN has less NO_x storage capacity

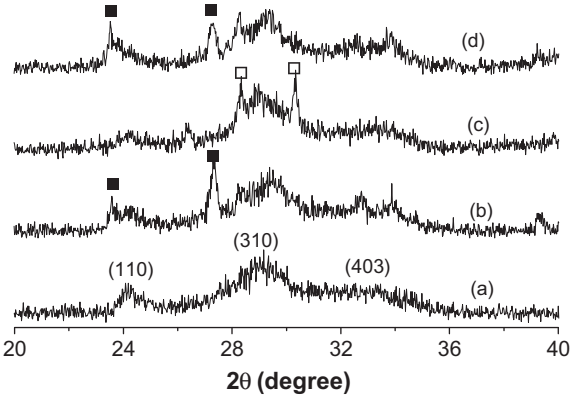

Fig. 10. XRD patterns: (a) KTN, and (b–d) Pt–26KNO_3/KTN; (b) as-prepared, (c) after reaction with H_2 reduction, and (d) after reaction with NO_x storage; ■ represent KNO_3 and □ represent K-rich titanate.

because of the low K/Ti ratio. The K/Ti ratio of the KTN-based catalysts was increased with the impregnation of KNO_3 (as shown in Table 2) and then the NO_x storage capacity increased. The ratio of NO_x/K was presented in Table 2, and the results showed that the ratio of potassium atoms acting as NO_x storage sites maximized to about 40% (when KNO_3 impregnated amount was 26–33%) and then decreased to 23% (when KNO_3 impregnated amount was 41%). Fig. 11 shows the possible schematic process of the NSR reaction on Pt–KNO_3/KTN catalyst. The impregnated H_2PtCl_6 and KNO_3 can be reduced during the pretreatment by H_2 reduction, and a K-rich layer on the nanobelt and Pt metallic particles can be formed. Once the impregnated KNO_3 amount on KTN increased, the thickness of K-rich layer increased; then the nanobelt structure finally

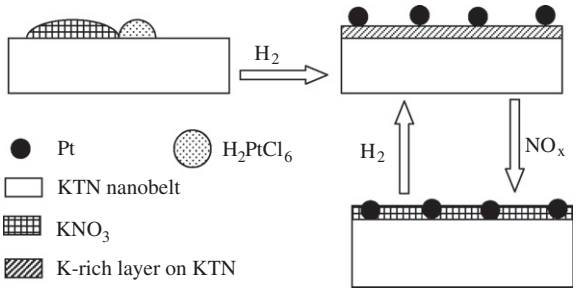

Fig. 11. Schematic procedure in NSR reaction over Pt–KNO_3/KTN catalyst.

transferred to a K-rich irregular structure similar to that of Pt–41KNO_3/KTN (Fig. 8d). During NO_x storage process, the NO was first oxidized on Pt to NO_2 and then combined with the K^+ from the K-rich layer to form KNO_3 on the surface. The formed NO_x storage species might easily move on the surface and finally cover the entire nanobelt surface, resulting in high NO_x storage capacity. During the NO_x reduction procedure, the formed KNO_3 was reduced and the K^+ moved back to the nanobelt to form a K-rich layer again.

4. Conclusions

In the present work, K-titanate with a nanobelt structure was prepared by hydrothermal method and examined as a catalyst support of Pt–KNO_3 for NSR reaction. The prepared catalysts exhibited high NO_x storage capacity (1.27–2.27 mmol/g) at 350 °C in the absence of CO_2. The maximal NO_x storage capacity (2.27 mmol) was the highest NO_x storage capacity ever reported in the relevant literatures. Combining the results of isothermal NO_x storage and lean–rich cycling experiment, as well as various characterizations of catalysts before and after reaction, we could demonstrate that the stored NO_x species KNO_3 covered the entire surface of the catalyst. The reduction of KNO_3 resulted in the formation of a K-rich layer on catalyst surface, and the immigration of K^+ from and back to K-rich layers might be the mechanism for the storage and reduction of NO_x on those materials. Maintaining the nanobelt structure and optimizing the amount of KNO_3 were the key factors to obtain high NO_x storage capacity. Although the prepared catalyst exhibits moderate stability at 350 °C with optimized amount of KNO_3 impregnation, operation at high temperature (such as 500 °C) would cause the destruction of catalyst during reaction. Improvement of the thermal stability should be addressed for the practical application of K-titanate nanomaterials as NSR catalysts.

Appendix A. Supplementary material

Supplementary data associated with this article can be found, in the online version, at doi:10.1016/j.jcat.2011.03.014.

References

[1] E.S.J. Lox, Handb. Heterog. Catal. 5 (2008) 2274.
[2] S. Roy, A. Baiker, Chem. Rev. 109 (2009) 4054.
[3] G. Centi, G.E. Arena, S. Perathoner, J. Catal. 216 (2003) 443.
[4] J. Kaspar, P. Fornasiero, N. Hicky, Catal. Today 77 (2003) 419.
[5] M. Iwamoto, S. Yokoo, K. Sakai, S. Kagawa, J. Chem. Soc., Faraday Trans. 77 (1981) 1629.
[6] N. Takahashi, H. Shinjoh, T. Suzuki, K. Yamazaki, K. Yokota, H. Suzuki, N. Miyoshi, S. Matsumoto, T. Tanizawa, T. Tanaka, S. Tateishi, K. Kasahara, Catal. Today 27 (1996) 63.
[7] S. Matsumoto, Catal. Today 29 (1996) 43.
[8] S. Matsumoto, Y. Ikeda, H. Suzuki, M. Ogai, N. Miyoshi, Appl. Catal. B: Environ. 25 (2000) 115.
[9] K. Tamazaki, T. Suzuki, N. Takahashi, K. Yokoda, M. Sugiura, Appl. Catal. B: Environ. 30 (2001) 459.
[10] P. Forzatti, Appl. Catal. A: Gen. 222 (2001) 221.
[11] G. Busca, L. Lietti, G. Ramis, F. Berti, Appl. Catal. B: Environ. 18 (1998) 1.
[12] M. Iwamoto, H. Yahiro, S. Shundo, Y. Yu-u, N. Mizuno, Appl. Catal. 69 (1991) L15–L19.
[13] K. Theinnoi, S. Sitshebo, V. Houel, R.R. Rajaram, A. Tsolakis, Energy Fuels 22 (2008) 4109.
[14] R. Burch, J.P. Breen, C.J. Hill, B. Krutzsch, B. Konrad, E. Jobson, L. Cider, K. Eränen, F. Klingstedt, L.-E. Lindfors, Top. Catal. 30–31 (2004) 19.
[15] F. Frola, M. Manzoli, F. Prinetto, G. Ghiotti, J. Phys. Chem. C 112 (2008) 12869.
[16] M. Happel, A. Desikusumastuti, M. Sobota, M. Laurin, J. Libuda, J. Phys. Chem. C 114 (2010) 4568.
[17] L. Lietti, P. Forzatti, I. Nova, E. Tronconi, J. Catal. 204 (2001) 175.
[18] N. Rankovic, A. Nicolle, P.D. Costa, J. Phys. Chem. C 114 (2010) 7102.
[19] T. Lesage, J. Saussey, S. Malo, M. Hervieu, C. Hedouin, G. Blanchard, M. Daturi, Appl. Catal. B: Environ. 72 (2007) 166.
[20] Y. Liu, M. Meng, Z. Zou, X. Li, Y. Zha, Catal. Commun. 10 (2008) 173.
[21] A. de Lucas, A. Caravaca, P. Sanchez, F. Dorado, J.L. Valverde, J. Catal. 259 (2008) 54.
[22] K. Yamamoto, R. Kikuchi, T. Takeguchi, K. Eguchi, J. Catal. 238 (2006) 449.
[23] Q. Wang, Z. Guo, J.S. Chung, Chem. Commun. (2009) 5284.
[24] Q. Wang, J.H. Sohn, J.S. Chung, Appl. Catal. B: Environ. 89 (2009) 97.
[25] X. Sun, Y. Li, Chem. A Eur. J. 9 (2003) 2229.
[26] Y. Lan, X. Gao, H. Zhu, Z. Zheng, T. Yan, F. Wu, S. Ringer, D. Song, Adv. Funct. Mater. 15 (2005) 1310.
[27] C. Tsai, H. Teng, Langmuir 24 (2008) 3434.
[28] D.V. Bavykin, J.M. Friedrich, A.A. Lapkin, F.C. Walsh, Chem. Mater. 18 (2006) 1124.
[29] X. Sun, X. Chen, Y. Li, Inorg. Chem. 41 (2002) 4996.
[30] V. Idakiev, Z.-Y. Yuan, T. Tabakova, B.-L. Su, Appl. Catal. A: Gen. 281 (2005) 149.
[31] L. Torrente-Murciano, A.A. Lapkin, D.V. Bavykin, F.C. Walsh, K. Wilson, J. Catal. 245 (2007) 272.
[32] T.A. Ntho, J.A. Anderson, M.S. Scurrell, J. Catal. 261 (2009) 94.